Electronic Supplementary Material (ESI) for RSC Advances.

Supporting Information

Hybrid Membrane Biomaterials from Self-Assembly in Polysaccharide and Peptide Amphiphile Mixtures: Controllable Structural and Mechanical Properties and Antimicrobial Activity

Valeria Castelletto, Amanpreet Kaur, Ian W. Hamley,* Ruth H. Barnes, Dr. Kimon-Andreas Karatzas

School of Chemistry, Pharmacy and Food Biosciences. University of Reading, Whiteknights, Reading RG6 6AD, United Kingdom.

Daniel Hermida-Merino

European Synchrotron Radiation Facility, ESRF, 71 avenue des Martyrs, 38000 Grenoble, France.

Steve Swioklo, Prof. Che J. Connon

Institute of Genetic Medicine, Newcastle University, International Centre for Life. Central Parkway, Newcastle upon Tyne NE1 3BZ, UK. Dr.

Joanna Stasiak

Department of Chemical Engineering and Biotechnology, Pembroke Street, Cambridge CB2 3RA, United Kingdom.

Dr. Mehedi Reza, Prof. Janne Ruokolainen

Department of Applied Physics, Aalto University School of Science, P.O. Box 15100 FI-00076 Aalto, Finland.

SAXS models. The SAXS intensity from a scattering object without a particular orientation can be approximated as the following equation:[1, 2]

$$I(q) \propto \left\langle F^2(q) S(q) \right\rangle \qquad (1)$$

where $F^2(q)$ is the scattering particle form factor and $S(q)$ is the interparticle interference function.

In this work we used several analytical expressions of the form factor to model the SAXS data. In particular, we used form factors for a Gaussian lipid bilayer, a spherical core and shell, a broad peak and a Guinier form factor. The Gaussian lipid bilayer and shell form factors were used to describe lamellar orders and micelles respectively. The broad peak and the Guinier form factors were used to describe amorphous structures.

The details of the Gaussian lipid bilayer model are given elsewhere.[3] Briefly, the model assumes an electron density profile comprising Gaussian functions for the head groups on either side of the bilayer and another Gaussian for the hydrocarbon chain interior. The midpoint of the bilayer is defined as $z = 0 = z_C$. In our model we assumed a Gaussian distribution of inter-head group thicknesses $2z_H$, with an associated degree of polydispersity Δ_{2z_H}. The fitting parameters of the model are the electron densities of the head group (ρ_H), the layer thickness z_H, the electron density of the hydrocarbon chains (ρ_C), the standard deviation of the position of the Gaussian peak at z_H (σ_H), the standard deviation of the position of the Gaussian peak at z_C (σ_C), and Δ_{2z_H}.

The spherical core and shell contribution was characterized by an overall radius of spherical shell (R_1), a radius of core (R_2) with an associated degree of polydispersity Δ_{R2}, a scattering length difference between shell and matrix (ρ), and a scattering length density difference between core and matrix relative to the shell contrast (μ).[4, 5]

The broad peak form factor depends on a characteristic distance between scattering inhomogeneities (Δ) and a length of correlation (ζ), while the Guinier from factor is characterized by the radius of gyration of the scattering object (R_G).

For liquid samples, the Gaussian lipid bilayer form factor was used together with the interference function *S(q)* (Eq. 1) corresponding to the modified Caillé theory appropriate for lamellar systems influenced by thermal fluctuations. Details of the model are given elsewhere,[6, 7] and will be omitted here. The structure factor *S(q)* is described by a series, which accounts for a diffuse background (N_{diff}) and the total number of layers *N*. Each term in the series depends on the layer thickness d_o and the Caillé parameter (η), which is a measure for the bilayer fluctuations.

For sacs and capsules, the Gaussian lipid bilayer form factor was used together with the interference function *S(q)* corresponding to a paracystalline structure factor describing weakly ordered membranes with a stacking disorder. As above, this structure factor is characterized diffuse background $N_{diff,p:}$; total number of layers N_p; stacking separation d_{op} and stacking disorder parameter η_p.

A hard sphere potential of interaction, with hard sphere radius R_H and hard sphere density ϕ, was used to describe the structure factor for the core and shell particles system. All fitting was done using the software SASfit.[8]

Table S1: Parameters extracted from the fitting of the SAXS data for sol II in Figure1c.

Sample / Parameter	Sample II
N1 [arb. units]	3.9×10^{-5}
Δ_{2zH} [Å]	5
$2z_H$ [Å]	28
σ_H [Å]	4
ρ_H [rel. units]	1.6×10^{-5}
σ_C [Å]	5
ρ_C [rel. units]	-4.2×10^{-6}
N [arb. units]	15
N_{diff}	2
d_o [Å]	42
η	0.6
N2 [arb. units]	14.1
R_1 [Å]	24.2
Δ_{R1} [Å]	3
R_2 [Å]	16.5
ρ [rel. units]	2.2×10^{-5}
μ [rel. units]	-0.82

Key: Gaussian bilayer form factor: scale factor N1, Gaussian half-width at half-maximum for polydispersity $\Delta_{2zH,}$ inter-head group thicknesses $2z_H$, Gaussian half-width for outer layer surface σ_H, electron density for headgroup ρ_H, Gaussian half-width for inner layer σ_C, relative electron density for inner layer ρ_C. **Caillé structure factor:** diffuse background $N_{diff.}$; total number of layers N; layer thickness d_o; Caillé parameter η. **Spherical shell form factor:** scale factor N2; overall radius of sphere R_1; radius of core R_2; Gaussian half-width at half-maximum for polydispersity Δ_{R1}, scattering lengths ρ and μ.

Table S2: SAXS parameters relevant to PA matrices and NaAlg solutions used to produce sol II, the membrane sac, cap I and cap II in Table 1.

Sample / Parameter	2 wt% C_{16}-KKFF	2 wt% C_{16}-KKFF (0.144 wt% $CaCl_2$)	5 wt% C_{16}-KKFF	0.3 wt% NaAlg	0.5 wt% NaAlg	2 wt% NaAlg (0.02 wt% GO)	2 wt% NaAlg (0.35 wt% GO)
N [arb. units]	12.17	12.7	23.6	--	--	--	--
R_1 [Å]	24.5	25.0	24.6	--	--	--	--
Δ_{R1} [Å]	3.5	3.4	3.3	--	--	--	--
R_2 [Å]	16.3	15.9	16.4	--	--	--	--
ρ [rel. units]	0.096	0.09	0.11	--	--	--	--
μ [rel. units]	-0.9	-1.13	-0.89	--	--	--	--
R_H [Å]	60.4	47	50.2	--	--	--	--
ϕ	0.17	0.1	0.25	--	--	--	--
Δ [Å]	--	--	--	161	146	89.7	96.6
ζ [Å]	--	--	--	26	26	26	4.7

Key: Spherical shell form factor: scale factor N; overall radius of spherical shell R_1; radius of core R_2; Gaussian half-width at half-maximum for polydispersity Δ_{R1}, scattering lengths ρ and μ. **Hard sphere interaction:** hard sphere radius R_H and hard sphere density ϕ. **Broad peak form factor:** distance between scattering inhomogeneities Δ and a length of correlation ζ.

Table S3: Parameters extracted from the fitting of the SAXS data for samples in Figure 4a.

Sample / Parameter	membrane sac	cap I	cap II
N [arb. units]	8.7	7	0.5
Δ_{2zH} [Å]	4.9	4.9	4.9
$2z_H$ [Å]	40	40	40
σ_H [Å]	0.64	0.64	0.64
ρ_H [rel. units]	9.6x 10^{-7}	9.6x 10^{-7}	9.6x 10^{-6}
σ_C [Å]	1.5	1.5	1.5
ρ_C [rel. units]	-1.4x 10^{-6}	-1.4x 10^{-6}	-2.7x 10^{-6}
N_p [arb. units]	27	25	8
$N_{diff,p}$	8.3	8	8
d_{op} [Å]	42	42.5	43.5
η_p	3.2	3.4	2.7
R_G [Å]	76.6	--	--

Key: Gaussian bilayer form factor: scale factor N, Gaussian half-width at half-maximum for polydispersity $\Delta_{2zH,}$ inter-head group thicknesses $2z_H$, Gaussian half-width for outer layer surface σ_H, electron density for headgroup ρ_H, Gaussian half-width for inner layer σ_C, relative electron density for inner layer ρ_C. **Paracrystalline structure factor:** diffuse background $N_{diff,p:}$; total number of layers N_p; stacking separation d_{op}; stacking disorder parameter η_p. **Guinier form factor.** R_G: radius of gyration.

Table S4: Origin of SAXS (Figure 1c and Figure 4a) and WAXS (Figure 5b) spacing for samples in Table 1.

Sample / Spacing	Sol II	Membrane sac	cap I	cap II	Origin
SAXS	42.8	42.8	42.8	44.5	Bilayer
WAXS	--	9.1	--	10.6	GO‡
	--	6.6	6.6	--	Na Alg‡
	--	--	5.2	5.9	GO‡
	--	4.4	4.4	--	PA*
	--	2.3	2.3	2.3	NaAlg‡
	--	--	--	2.1	GO‡

Based on ‡XRD data in Figure S5 and *single reflexion measured at 4.39 Å for 1 wt% C_{16}-KKFF.[9]

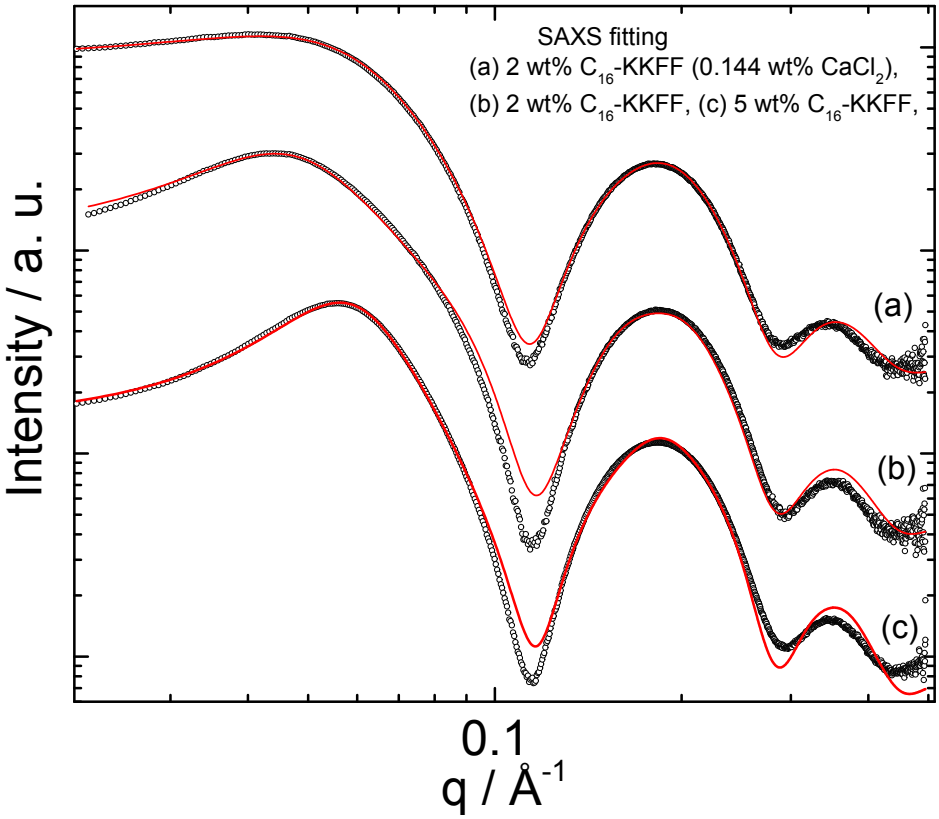

Figure S1. SAXS data and fitting for PA solution control samples. The SAXS data is fitted according to a spherical core-shell form factor and a hard sphere structure factor (parameters listed in Table S2).

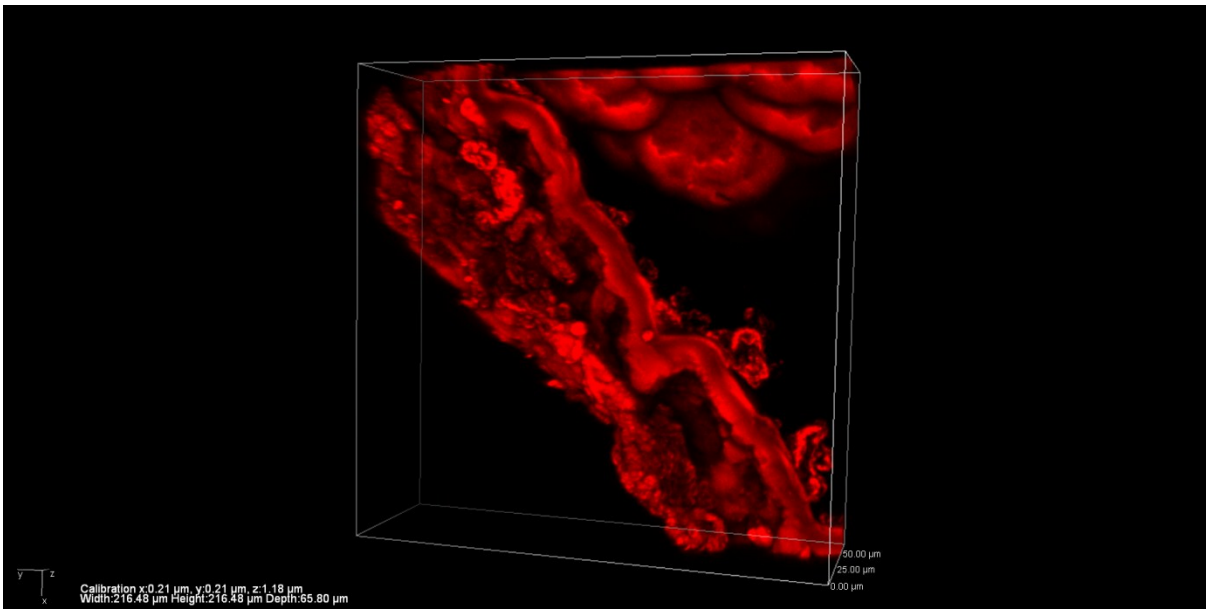

Figure S2. Laser scanning confocal microscopy image showing a cross section of the wall for the membrane sac stained with Rho B.

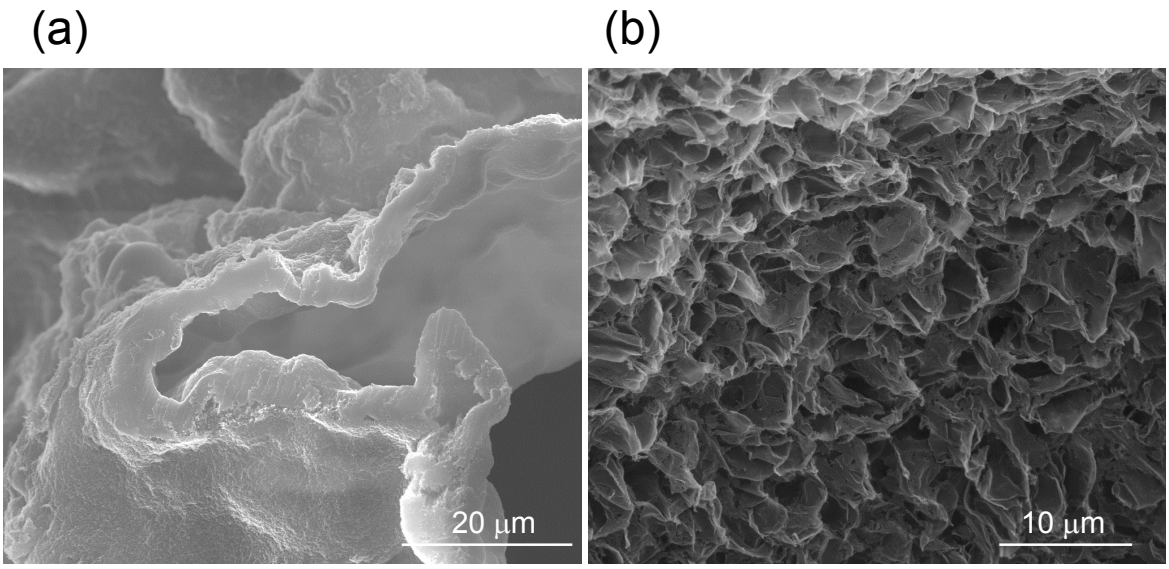

Figure S3. SEM images (a) cross section of the wall of cap I, (b) internal structure within a cap II.

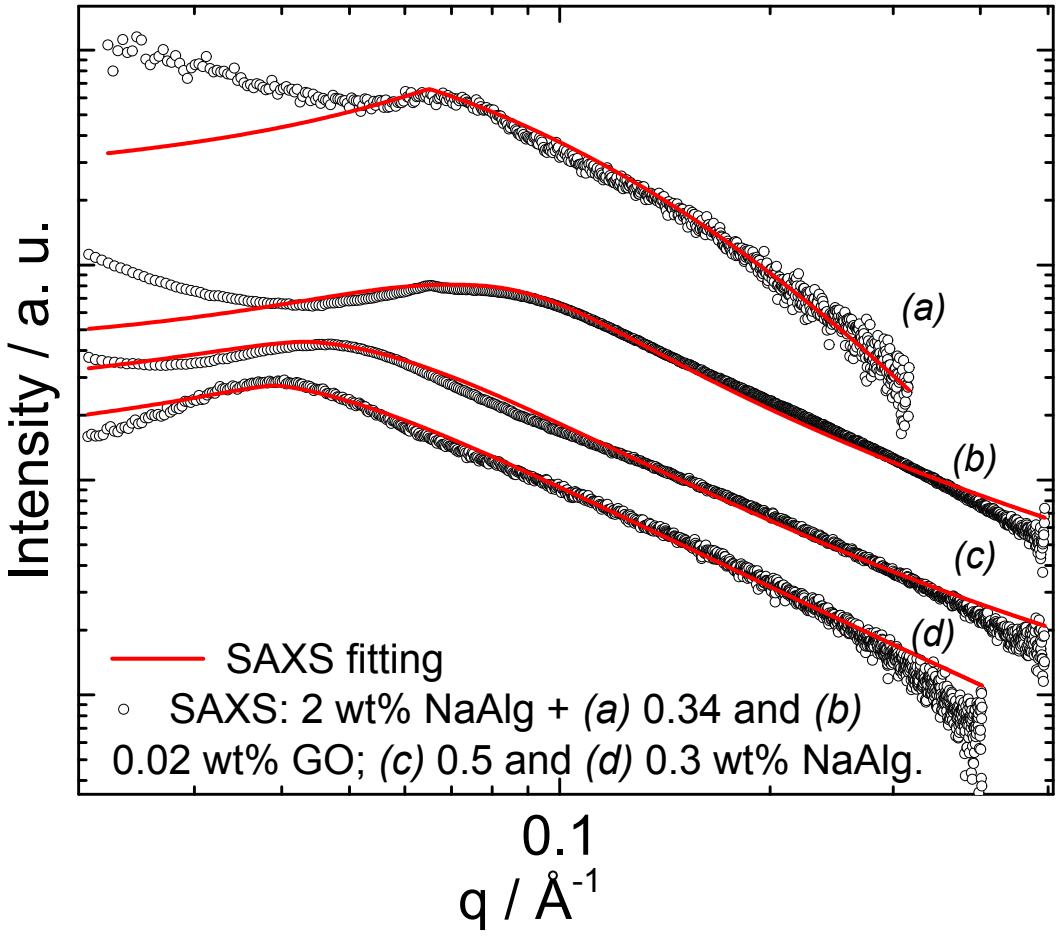

Figure S4. SAXS data and fitting for samples of sodium NaAlg with and without GO under the conditions shown. The SAXS data is fitted according to a broad peak (parameters listed in Table S2).

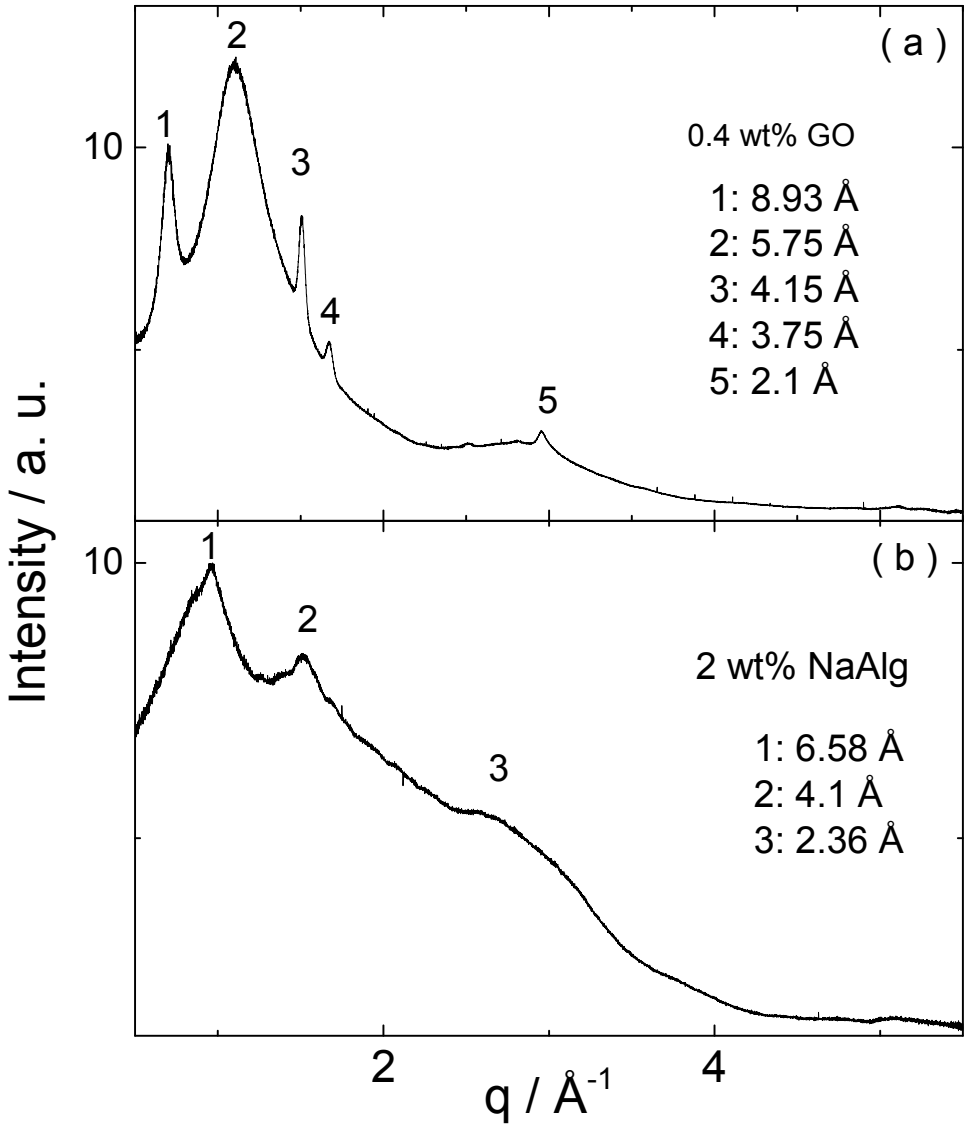

Figure S5. WAXS data from (a) 0.4 wt% GO and (b) 2 wt% NaAlg.

Figure S6. Caps I after staining with solutions of (left) the anionic dye Congo red and (right) the cationic dye Rho B. Only the capsule on the right adsorbed the staining solution.

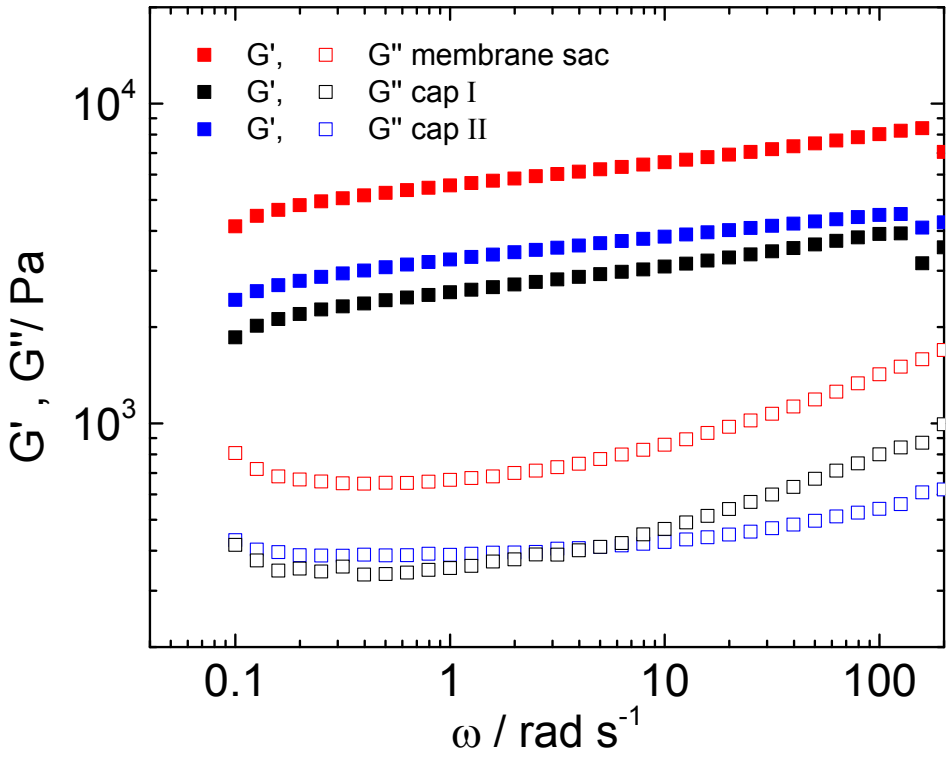

Figure S7. Frequency sweep experiments measured within the linear viscoelastic regime for the membrane sac, cap I and cap II, using oscillatory stress 90 Pa (membrane sac and cap I) or 30 Pa (cap II).

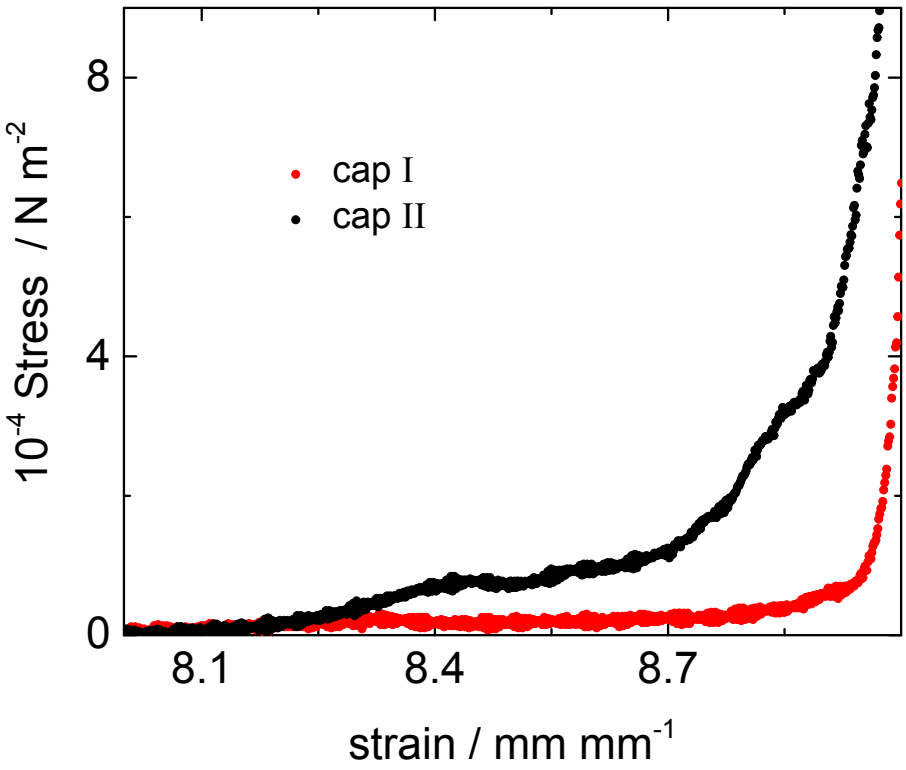

Figure S8. Texture analysis for cap I and cap II.

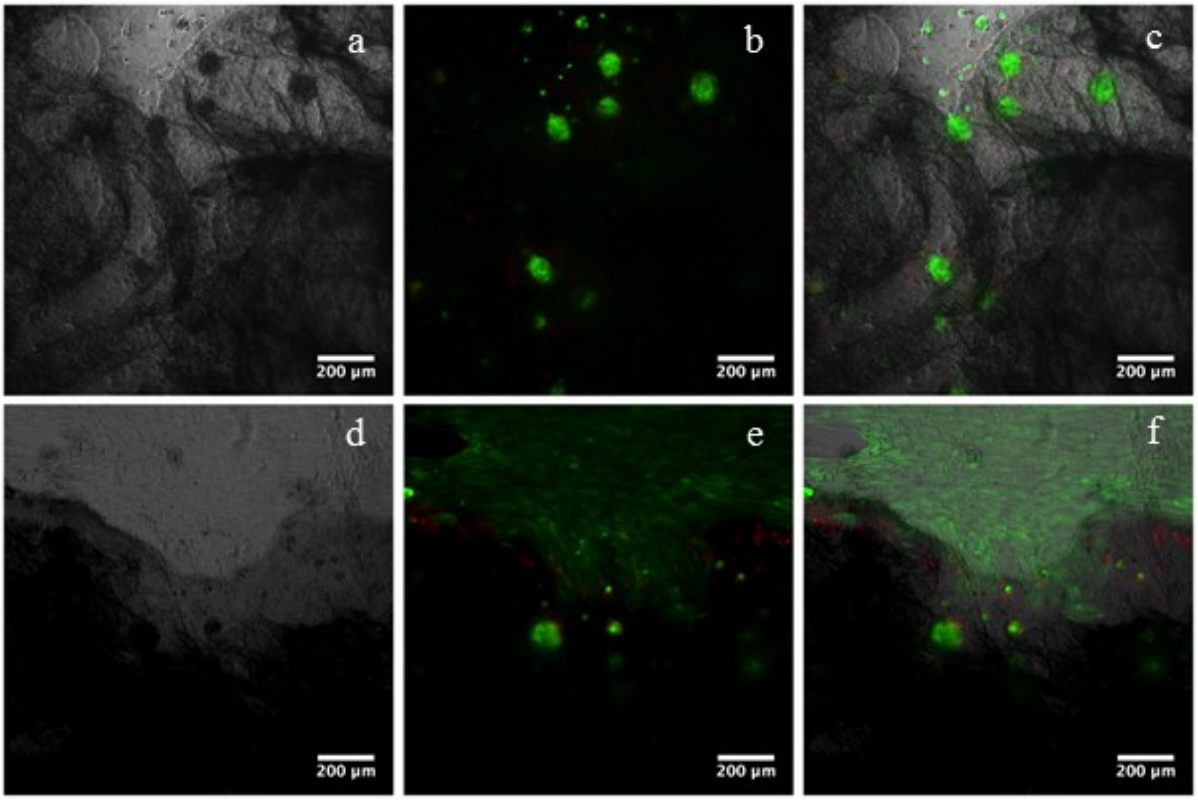

Figure S9. Biocompatibility testing after 7 days of films made from cap I modified by addition of C_{16}-G_3RGD. 24 hours after seeding, hASCs were stained with calcein-AM (live indicator; green) and ethidium homodimer-1 (dead indicator; red) before capturing images by fluorescent microscopy.

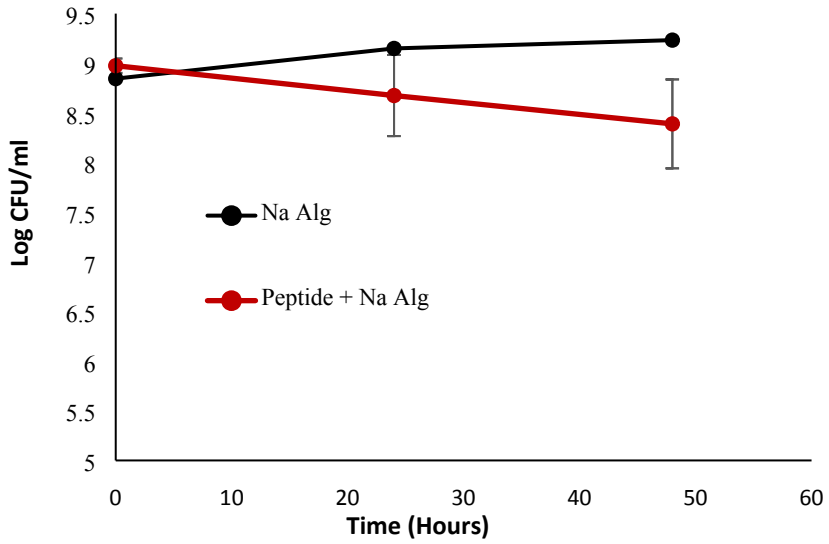

Figure S10. Survival of *E. faecalis* after exposure to the presence (red points) or absence (black points) of the peptide in the liquid phase. Estimations of the cell numbers (CFU: colony-forming units) at each time point were performed in triplicate (3 biological replicates) while each dilution was plated in duplicate (2 technical replicates). Markers represent an average of the measurements performed in triplicate, and error bars represent the standard deviation.

References

1. J. S. Pedersen and C. Svaneborg, *Curr. Opin. Colloid Interface Sci.*, 2002, **7**, 158-166.
2. V. Castelletto and I. W. Hamley, *Curr. Opin. Colloid Interface Sci.*, 2002, **7**, 167-172.
3. G. Pabst, M. Rappolt, H. Amenitsch and P. Laggner, *Phys. Rev. E*, 2000, **62**, 4000-4009.
4. J. S. Pedersen, *Advances in Colloid and Interface Science*, 1997, **70**, 171-210.
5. J. S. Pedersen, *Curr. Opin. Colloid Interface Sci.*, 1999, **4**, 190-196.
6. R. Zhang, R. M. Suter and J. F. Nagle, *Phys. Rev. E*, 1994, **50**, 5047-5060.
7. M. Caillé, *C. R. Acad. Sci. Paris*, 1972, **274**, 891-893.
8. I. Breßler, J. Kohlbrecher and A. F. Thünemann, *Journal of Applied Crystallography*, 2015, **48**, 1587-1598.
9. A. Dehsorkhi, I. W. Hamley , J. Seitsonen and J. Ruokolainen, *Langmuir*, 2013, **29**, 6665-6672.